Life of thermal bubble on platinum microheater

Ho-Young Kim[a] and Kwang-Hun Jeong
School of Mechanical and Aerospace Engineering, Seoul National University, Seoul 151-744, Korea

Seunghyun Ko, Heon Ju Lee, Yoon Pyo Lee, and Young Soo Chang
Thermal/Flow Control Research Center, Korea Institute of Science and Technology, Seoul 136-791, Korea

(Received 27 September 2006; accepted 26 June 2007; published online 9 August 2007)

When electrical current is supplied to a microline heater immersed in liquid, a microthermal bubble can be formed. The bubble grows until it becomes too large to adhere to a solid surface and finally departs into liquid completing its life. Here we report the experimental results associated with the life of a thermal bubble continuously heated by a platinum microheater. We investigated the effects of the heater dimensions on the nucleation temperature. It was found that a bubble nucleates at lower temperature as the heater gets wider. We also measured the departure diameter and frequency of thermal bubbles depending on the thermal conditions of the microheater and the ambient liquid. As the microheater temperature increases, both the departure diameter and frequency increase, showing different behaviors from those of macroscale boiling. However, as the ambient liquid temperature rises, the departure diameter decreases despite the increase of the departure frequency. Finally, the transient temperature profile of the microheater during bubble formation process was measured. Rapid drop and rise of the temperature were observed, which are attributed to the small-scale convection of cold ambient liquid. © *2007 American Institute of Physics*.
[DOI: 10.1063/1.2767862]

I. INTRODUCTION

Creating and manipulating thermal bubbles using microheaters is one of the most important areas in microfluidics. Microelectromechanical system (MEMS) technology based on thermal bubbles enjoyed a huge commercial success in the ink-jet printing market for decades. These days, attempts are being made to use microbubbles in other applications, such as microactuation,[1] micropump/mixer,[2,3] and biosample delivery.[4] For the aforementioned technical applications, understanding diverse bubble behavior, including its formation, growth, and departure, on microheaters is essential. In addition, the advantage of a microline heater of allowing for the creation and observation of a single thermal bubble can be utilized to advance the fundamental understanding of general boiling heat transfer phenomena.

The configurations of microheaters used to generate bubbles are classified into two categories, i.e., planar and line heaters. The planar heater, adopted in ink-jet print heads, is an array of linear resisters. Reference 5 measured the temperature evolution of the ink-jet heater, powered by a pulsed input, using a sophisticated bridge circuit. Also an imaging technique based on a laser strobe microscopy to record nucleation and growth of microbubbles formed on pulse-heated planar heaters was developed.[6,7] Further, nanobubbles on a hydrophilic microplanar heater were inferred using two consecutive heat pulses.[8] In general, very small bubbles are nucleated at multiple sites on the planar heater and they grow to coalesce into a large bubble.[9,10] On the other hand, a single bubble is nucleated and grows on microline heaters.[11] Either a pulsed current input or a continuous current supply can be employed to power the microline heater to generate thermal bubbles. Nucleation temperature of a bubble on a polysilicon line heater induced by a current pulse typically shorter than 0.1 s was measured by Lee *et al.*[12] They found the nucleation temperature on a 3-μm-wide heater to be higher than the liquid's superheat limit but that on a 5-μm-wide heater to be lower than the superheat limit. The generated bubble condenses back to liquid while keeping its contact with the heater when the power is shut off. On the other hand, the bubble formed on a continuously heated line heater continues to grow until its departure.[11] Tsai and Lin[13] modeled the transient bubble diameter and temperature change during the growth of a single bubble on a line heater using first-order approximations.

When current is supplied continuously to a microheater, one can observe microthermal bubbles form, grow, and depart repeatedly. Although not explored in practical applications yet, this phenomenon corresponds to the conversion of a dc input (constant voltage) to an ac output (periodical bubble generation). For example, if a flexible structure is situated near the heater, a continuous current input to the heater may induce the periodic deformation of the solid structure in a similar manner to Ref. 1. Therefore, here we are interested in characterizing thermal history of a bubble on a microline heater, covering its birth (formation), death (departure), and rebirth (subsequent formation), when the continuous current is supplied. We visualize the bubble behavior using a high-speed imaging system while simultaneously measuring the heater temperature. As for the birth of a microbubble, we report the measurement results of the nucleation temperature for different dimensions of microline

[a]Author to whom correspondence should be addressed; electronic mail: hyk@snu.ac.kr

 © 2007 American Institute of Physics

Downloaded 10 Aug 2007 to 147.46.245.171. Redistribution subject to AIP license or copyright, see http://jap.aip.org/jap/copyright.jsp

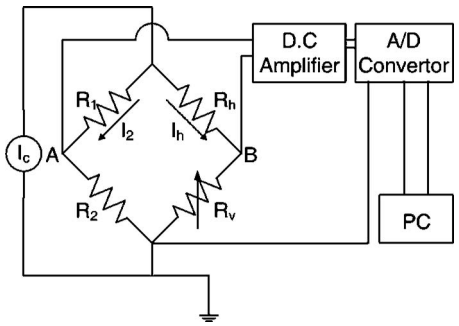

FIG. 1. Bridge circuit to measure the transient heater temperature.

heaters. The bubble behavior associated with its death is studied by way of measuring the departure frequency and diameter. The transient heater temperature profile upon bubble rebirth is also reported.

II. EXPERIMENTS

We fabricated platinum microline heaters on a 700-μm-thick Pyrex wafer using microfabrication technology. After depositing titanium as adhesion layer, platinum was deposited by e-beam evaporation. Patterned heaters of the 200 nm thickness was obtained by the advanced oxide etching (AOE) process. Since Pyrex is an insulating material, no process is necessary to deposit an insulation layer. A patterned platinum heater needs no additional deposition of metal contact pad. Therefore, the fabrication of the heater chip is relatively simple as compared with that of polysilicon microheaters on a silicon wafer.[11]

Various dimensions of heaters were made to examine the effects of heater sizes. The heater lengths varied as 100, 300, and 500 μm, and for each length of the heater, three different widths of 5, 10, and 20 μm were employed. Platinum is an ideal material to measure its temperature by reading its electrical resistance because it has the following linear resistance-temperature relationship:[14]

$$R_h = R_0[1 + \xi(T_h - T_0)], \tag{1}$$

where R_h and R_0 are the heater resistances at the temperatures T_h and T_0, respectively. The coefficient of linear proportionality ξ is dependent on the film deposition condition, thus was calibrated for each heater. The typical value of ξ was measured to be about 0.0033 K^{-1}. The Wheatstone bridge circuit as illustrated in Fig. 1 was constructed to measure the heater resistance R_h while providing a constant current I_c to the heater. In the figure, R_1 and R_2 are the reference resistances, and R_v is the variable resistance that is set to make the voltage difference of A and B zero when no current is supplied. As the current is supplied, the heater resistance changes, giving rise to the difference in voltage at A and B, $V_A - V_B$. We measure this voltage difference by an A/D (analog/digital) converter at the maximum sampling rate of 300 Hz. The heater resistance is obtained by the following formula:[14]

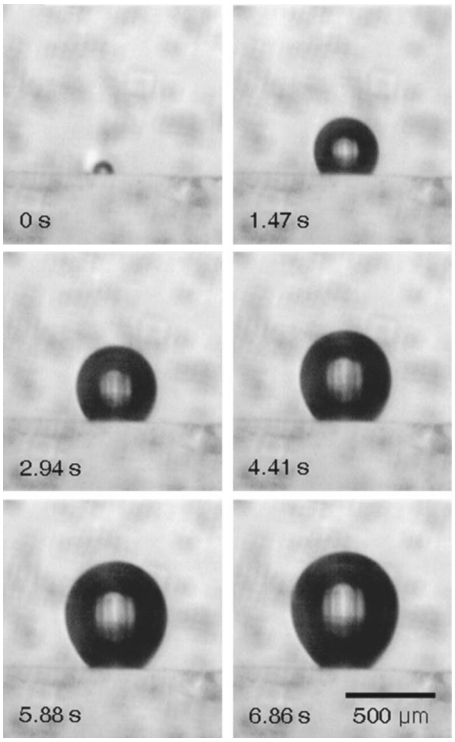

FIG. 2. Images of a thermal bubble on a platinum microline heater of the length of 100 μm and the width of 5 μm. The average heater temperature is 156 °C.

$$R_h = \frac{R_1 R_v I_c + (R_1 + R_2 + R_v)(V_A - V_B)}{R_v I_c - (V_A - V_B)}. \tag{2}$$

The heater temperature is obtained from the measured heater resistance using Eq. (1). The experimental uncertainty[15] associated with the heater temperature measurement as described above is within approximately ±3%.

As a working fluid, FC-72 was used because it is electrically insulating thus is free of electrolysis bubbles when electrical voltage is applied. The microheater chip was immersed in a liquid bath. The bulk temperature of liquid was controlled using a heater situated inside the vessel. One sidewall of the vessel was made of acrylic to provide optical access to the bubbles. The bubble behavior was imaged using a high-speed charge coupled device (CCD) camera (Redlake PCI 2000S) to obtain the transient size evolution and the departure frequency of the bubbles. The images taken by the camera consist of 480×420 and 240×92 pixels when operated at 60 and 2000 frames/s, respectively. Figure 2 shows the typical sequence of images from bubble formation until departure taken by the CCD camera operated at 60 frames/s with an objective lens (Computar 10× macrolens). In the lowest resolution mode, the error associated with the bubble size measurement is within ±8 μm.

III. RESULTS AND DISCUSSION

A. Nucleation temperature and heater dimensions

We investigated how the heater dimensions affect the temperature at which thermal bubbles first appear. Such consideration is of a critical importance in designing practical microsystems having a high bubble-generation efficiency.

Downloaded 10 Aug 2007 to 147.46.245.171. Redistribution subject to AIP license or copyright, see http://jap.aip.org/jap/copyright.jsp

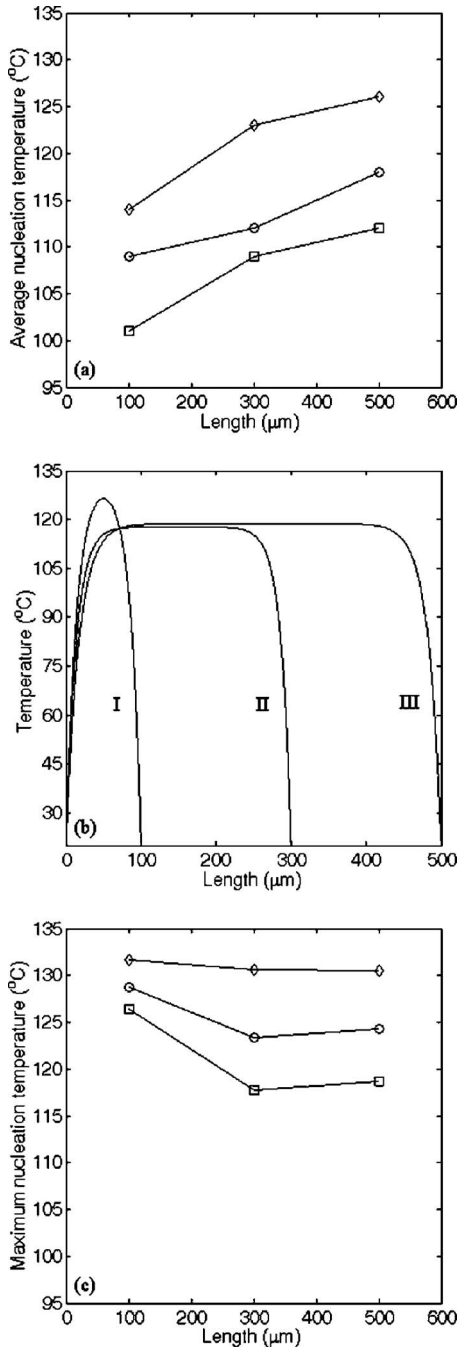

FIG. 3. Effects of heater dimensions on bubble nucleation temperature. (a) Average nucleation temperature of the heaters having the width of 5 μm (diamonds), 10 μm (circles), and 20 μm (squares) vs length. (b) Temperature profile along the 20-μm-wide microline heaters having the lengths of 100 μm (line I), 300 μm (line II), and 500 μm (line III). (c) Peak temperature at the nucleation onset in the heaters having the widths of 5 μm (diamonds), 10 μm (circles), and 20 μm (squares) vs length.

The experiments were performed with the ambient liquid temperature set to be 20 °C. Figure 3(a) shows the average heater temperature at the nucleation onset, as deduced from the heater resistance, depending on the width and length of the microline heaters. The experimental results reveal that as the heater width increases, the average nucleation temperature decreases. However, as the heater gets longer, the average nucleation temperature increases.

While the average heater temperature indicates how much electric power needs to be supplied to give rise to bubble nucleation, the actual bubble nucleation is more likely to be governed by the peak temperature at the heater center. The temperature profile in the microline heater can be obtained using the model of Lin and Pisano.[16] Although the detail of the model is not repeated here, it yields the temperature profile along the microline heater by solving the energy balance equation which includes joule heating, heat conduction through the substrate and along the line heater, and convection to the surrounding liquid. The modification made for this work is that the heat conduction from the bottom of line heater to the Pyrex wafer was modeled as a semi-infinite solid, while the Lin and Pisano model assumed that the entire temperature drop occurs in a thin insulating layer between the heater and the silicon wafer. Thus obtained temperature profiles at the nucleation onset in the microline heaters of 20 μm width but of various lengths are shown in Fig. 3(b). It is interesting to note that the heaters longer than 100 μm have wide peak temperature range, while a short heater of the length of 100 μm exhibits a sharp temperature peak. Similar trends are observed in the heaters of the other widths of 5 and 10 μm.

Such temperature profiles lead to the following consideration of the heat conduction along the line heater that gives rise to the lengthwise temperature variation. The heat transfer model indicates that most of the power supplied to the heater is conducted to the Pyrex substrate through the heater's bottom area lw, where l and w are the heater length and width, respectively. If the total power supplied to the heater is denoted by q_t, the heat loss through the cross section (of the area tw) of the heater q_c can be estimated as $q_c \sim (t/l)q_t$, where t is the heater thickness. Assuming that thermal gradient occurs over the distance δ in the lengthwise direction, a scaling estimate for the conduction along the line heater is written as $q_c \sim 2ktw\Delta T/\delta$, where k is the thermal conductivity of the platinum. Using the representative values for k =72 W/m/K, w=20 μm, l=300 μm, ΔT=100 K, and q_t =40 mW, δ is given by 20 μm, whose order of magnitude agrees with the length range, where temperature gradient occurs in Fig. 4(b). Therefore, for the heaters much longer than 2δ, the flat peak temperature range exists. For the heaters having the length of the same order as 2δ, the nonzero temperature gradient exists for the entire length.

As Fig. 3(c) indicates, our experiments indicate that when the heater lengths are 300 and 500 μm, the maximum temperature of the heater at the nucleation onset is rather insensitive to the heater length and lower than that of the shorter heaters of the length of 100 μm. The fact that a plateau of peak temperature exists for the heaters of the lengths of 300 and 500 μm may be related to the insensitivity of the nucleation temperature of the heaters of that length range, but a further study is required to theoretically explain the trend found in Fig. 3(c). We also note that wider heaters are experimentally shown to induce bubble nucleation at lower temperature than those of narrower heaters of the same length. The observations suggest that the maximum heater temperature for bubble nucleation tends to be lower when a large area is heated for the same heater length. Thus, it is possible to infer that large heaters can easily heat up more area to increase the number of superheated molecule clusters

Downloaded 10 Aug 2007 to 147.46.245.171. Redistribution subject to AIP license or copyright, see http://jap.aip.org/jap/copyright.jsp

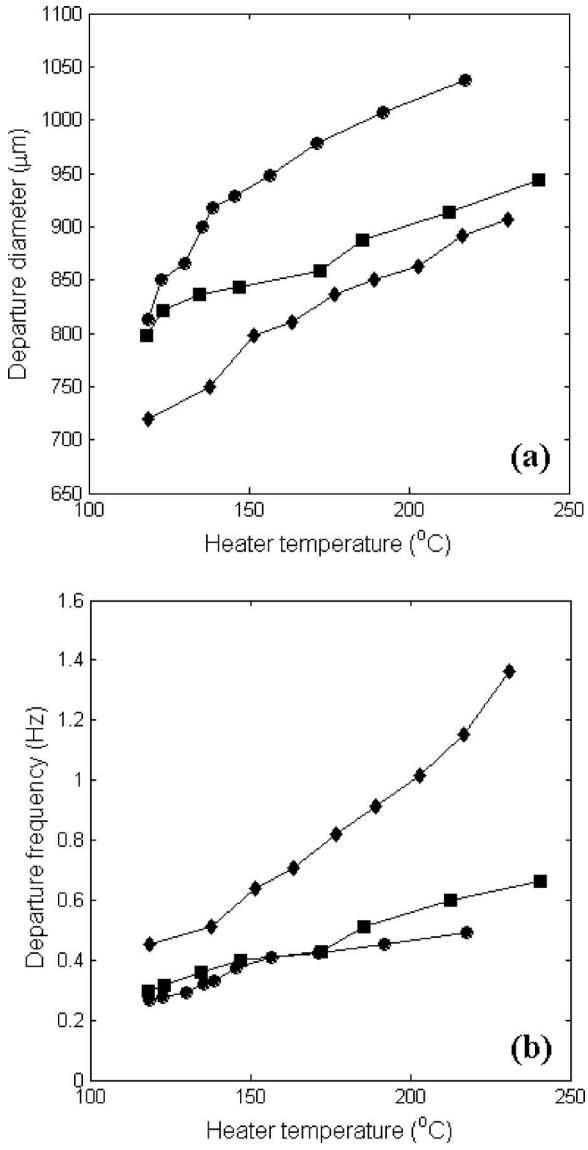

FIG. 4. Effects of the heater temperature and the ambient liquid temperature on (a) the departure diameter and (b) the departure frequency of bubbles. Circles, squares, and diamonds correspond to the ambient liquid temperatures of 20, 28, and 35 °C, respectively.

ready to vaporize, thus lowering the nucleation temperature. The increase in average nucleation temperature with the increase of heater length, as shown in Fig. 3(a), appears to be related to the fact that the portion of the maximum temperature plateau region of the entire heater length increases as the heater length increases. For instance, in Fig. 3(b), the average temperature is the highest for the longest heater (III) although the peak temperature is the highest for the shortest heater (I). With the current heater dimensions and heating rates, the maximum temperature in the heater at the nucleation onset ranges from about 117 to 133 °C, which is substantially higher than the boiling point of FC-72 at an ambient pressure (56 °C). However, it is considerably lower than the superheat limit of the liquid (148 °C),[17] indicating that heterogeneous nucleation occurred.

B. Diameter and frequency of bubble departure

Once nucleated, the bubble grows until its size gets large enough to overcome the surface tension force that holds it to the heater surface. The size of bubbles at departure and their departure frequency were measured for various thermal conditions of the heater and of the ambient liquid. Figure 4 summarizes the measurement results for the microheater having the length of 500 μm and the width of 10 μm. As the heater temperature increases, both the departure diameter and the departure frequency increase. On the other hand, as the ambient liquid temperature increases, the departure diameter decreases but the departure frequency increases. Here the departure diameter indicates the maximum diameter at the bubble equator before its contact area with the substrate rapidly reduces.

In macroscale boiling experiments, as the substrate temperature rises, the departure frequency increases, while the departure diameter decreases.[18] However, our experiments with microline heaters reveal that the increase of heater temperature increases both the departure diameter and frequency. When there is no external disturbance and the temperature dependence of the fluid properties and dynamic effects are ignored, the departure diameter of the bubble should be the same regardless of the substrate temperature. It is because the departure is determined merely by the balance of buoyancy and surface tension. However, it is apparent that the thermal and dynamic conditions of the bubble's neighbor exert a profound effect on the departure diameter. To understand such observations, we measured the temporal evolution of the contact diameter of bubble and heater surface since the contact diameter can indicate the relationship between the heater temperature and the bubble size effectively.

As shown in Fig. 5(a), the contact diameter increases faster as the heater temperature increases. Once the contact diameter reaches the maximum, it plateaus until a rapid drop takes place. Because the bubble growth is driven by the evaporation of microlayer near the heater surface, the departure diameter is determined by the amount of evaporation before the departure occurs. The experimental results show that the higher heater temperature increases the area where evaporation occurs, thus, the amount of vapor supply. This appears to be the major difference between the boiling on microline heaters and the macroboiling where the entire area is heated over the saturation temperature. Rapid drops of contact diameter observed in Fig. 5(a) correspond to the departure of bubbles. Rapidly grown, larger bubbles are more vulnerable to the buoyant effects of the surroundings than slowly grown, smaller bubbles, thereby having higher departure frequency.

The effects of the ambient liquid temperature on the departure diameter and frequency are of the same tendency as that of macroboiling. Figure 5(b) shows the temporal evolution of contact diameter under different ambient liquid temperatures. Here the electrical power supplied to the heater was the same (48 mW) for all the cases. The transient behavior of the contact diameter is similar for all the cases due to the same heat flux from the heater. However, the contact diameter starts to drop earlier as the ambient liquid temperature increases. A close observation of the high-speed images revealed that the perturbation on the bubble surface was more vigorous as the ambient liquid temperature increases. Therefore, bubbles surrounded by a hotter liquid tend to de-

Downloaded 10 Aug 2007 to 147.46.245.171. Redistribution subject to AIP license or copyright, see http://jap.aip.org/jap/copyright.jsp

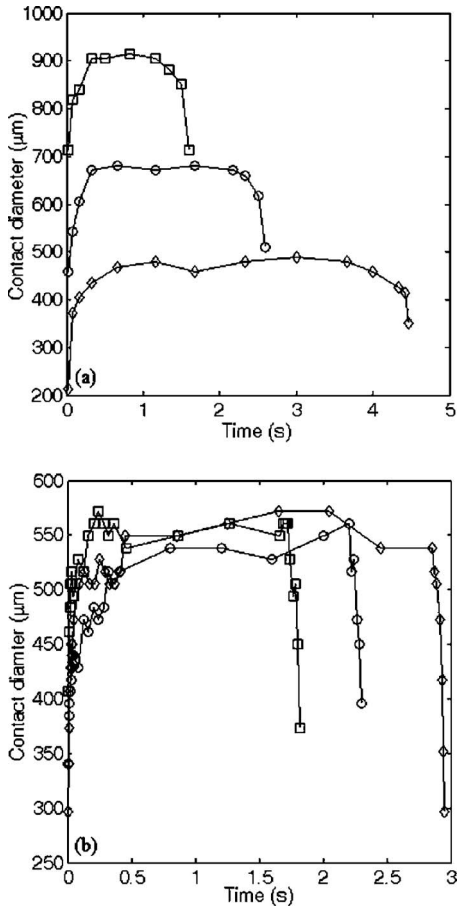

FIG. 5. Transient profile of the bubble contact diameter for different (a) heater temperatures and (b) ambient liquid temperatures. In (a), diamonds, circles, and squares correspond to the heater temperatures of 111, 145, and 256 °C, respectively. In (b), diamonds, circles, and squares correspond to the ambient liquid temperatures of 20, 28, and 35 °C, respectively. In all the cases, the microheater is 500 μm long and 10 μm wide.

part from the substrate more easily, resulting in a higher departure frequency. For lower ambient liquid temperature, the bubble stays in contact with the heater for a longer time, thus more evaporation can take place. This explains the increase of departure diameter with the decrease of ambient liquid temperature.

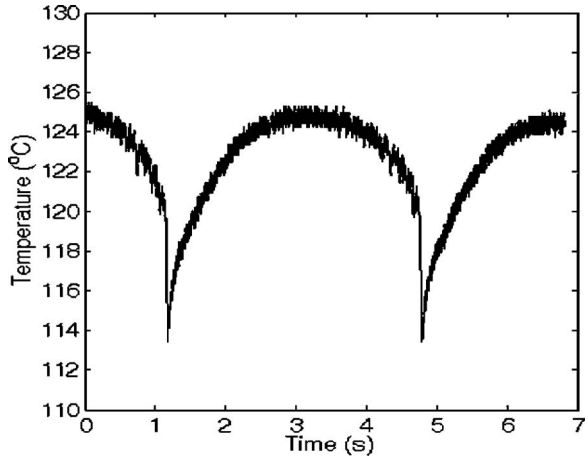

FIG. 6. Temporal evolution of microheater (500 μm long and 10 μm wide) temperature associated with the repeated process of bubble nucleation, growth, and departure.

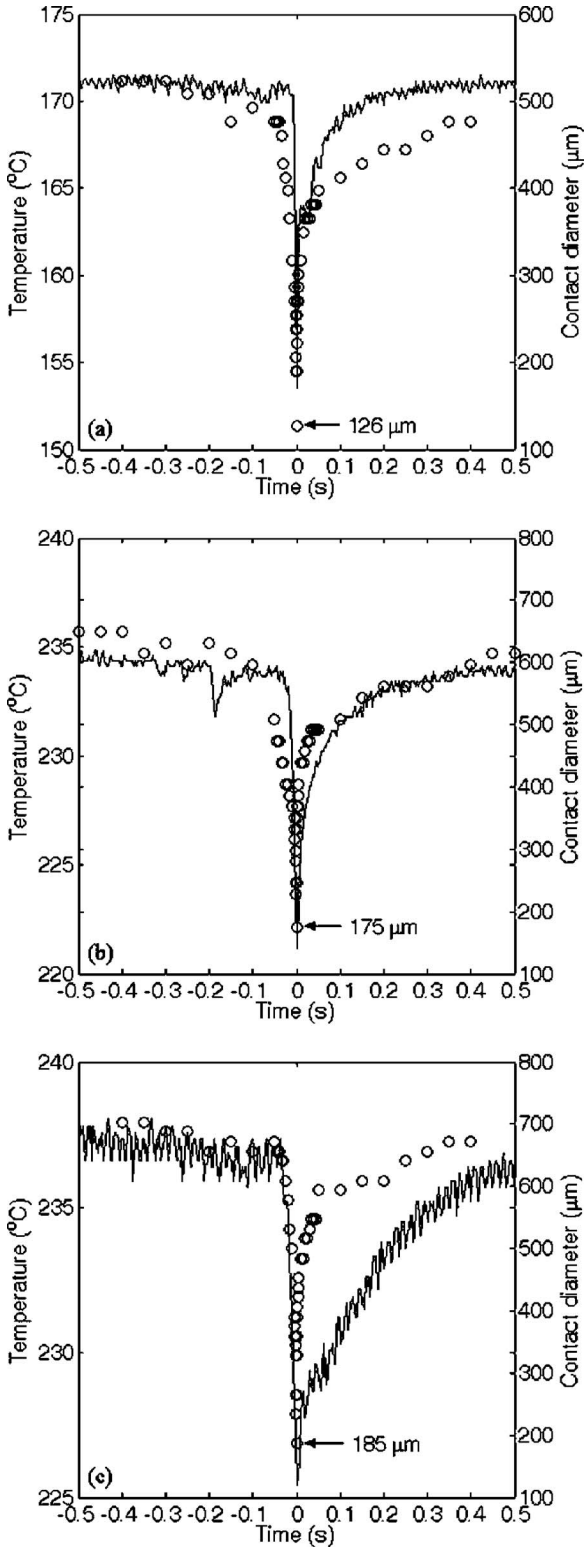

FIG. 7. Temporal evolution of microheater temperature (solid lines) and bubble contact diameter (circles) around the instant of bubble departure. The microheaters are commonly 5 μm wide but (a) 100 μm, (b) 300 μm, and (c) 500 μm long.

C. Periodic fluctuation of microheater temperature

To investigate the heat transfer phenomena associated with the microbubble growth and departure in steady operation, the heater temperature was measured using the A/D converter of the sampling rate of 300 Hz. Figure 6 shows

Downloaded 10 Aug 2007 to 147.46.245.171. Redistribution subject to AIP license or copyright, see http://jap.aip.org/jap/copyright.jsp

that the heater temperature repeats rapid drop and rise periodically, and the temperature difference during the process reaches over 10 °C. We find the period to be identical to the lifetime of a bubble on the substrate. Therefore, it is natural to associate such downward peak of the temperature with the bubble departure and the subsequent nucleation.

We overlapped the transient temperature profile with the bubble/substrate contact diameter in Fig. 7 for different lengths of the heaters. The contact diameter was measured using the images from the high-speed camera operated at 2000 frames/s. It is evident that the temperature drop is related to the decrease of the contact diameter prior to the bubble departure. That is, as the bubble is about to rise decreasing its contact area with the substrate, cold liquid surrounding the bubble is drawn into a region close to the heater. Hence the heater is momentarily cooled.

In Fig. 7, we set the instants when the minima of temperature and the contact diameter occur to be zero together. In Fig. 7(a), the temperature rises faster than the contact diameter. However, for longer heaters of Figs. 7(b) and 7(c), the contact diameter rises faster than the temperature. This difference is explained by comparing the minimum contact diameter and the heater length. As indicated in each figure, the minimum contact diameter (126 μm) of Fig. 7(a) is still greater than the heater length (100 μm). Hence the heater is always surrounded by vapor throughout the bubble formation-departure process. Therefore, the heater can be heated up again rapidly without losing heat to the ambient liquid that has a higher thermal effusivity than that of vapor. However, for longer heaters, the heaters are partly exposed to the ambient liquid when the contact area shrinks. Therefore, the heater temperature rises relatively slowly due to increased heat loss to the liquid.

IV. CONCLUSIONS

In this work, we studied the heat transfer process associated with the formation and departure of microbubbles on microline heaters. We investigated the effects of the heater dimensions on the nucleation temperature. It was found that a bubble nucleates at lower average temperature as the heater gets wider and shorter. However, the temperature peak in the heater is lower for longer heaters when the widths are the same. We also measured the departure diameter and frequency of thermal bubbles depending on the thermal conditions of the microheater and the ambient liquid. It was found that as the microheater temperature, or heat flux, increases, both the departure diameter and frequency increase. However, as the ambient liquid temperature rises, the departure diameter decreases despite the increase of the departure frequency. Finally, the transient temperature profile of the microheaters during bubble formation process was measured. Rapid drop and rise of the temperature were observed, which is attributed to the small-scale convection of cold ambient liquid.

ACKNOWLEDGMENTS

The authors are grateful to the Korea Research Council of Fundamental Science and Technology and KIST for the support of this work. One of the authors (H.Y.K.) also acknowledges administrative support from Institute of Advanced Machinery and Design at Seoul National University.

[1] L. Lin, A. P. Pisano, and A. Lee, Proceedings of the IEEE Transducers, 1991, pp. 1041–1044.
[2] J.-H. Tsai and L. Lin, Proceedings of the IEEE MEMS Workshop, 2001, pp. 409–412.
[3] L. Lin and J.-H. Tsai, Sens. Actuators, A **97/98**, 665 (2002).
[4] R. B. Maxwell, A. L. Gerhardt, M. Toner, M. L. Gray, and M. A. Schmidt, J. Microelectromech. Syst. **12**, 630 (2003).
[5] C. T. Avedisian, B. Osborne, F. D. McLeod, and C. Curley, Proc. R. Soc. London, Ser. A **455**, 3875 (1999).
[6] K. M. Balss, C. T. Avedisian, R. E. Cavicchi, and M. J. Tarlov, Langmuir **21**, 10459 (2005).
[7] C. T. Avedisian, R. E. Cavicchi, and M. J. Tarlov, Rev. Sci. Instrum. **77**, 063706 (2006).
[8] R. E. Cavicchi and C. T. Avedisian, Phys. Rev. Lett. **98**, 124501 (2007).
[9] Y. Hong, N. Ashgriz, and J. Andrews, J. Heat Transfer **126**, 259 (2004).
[10] Z. Yin, A. Prosperetti, and J. Kim, Int. J. Heat Mass Transfer **47**, 1053 (2004).
[11] L. Lin, A. P. Pisano, and V. P. Carey, J. Heat Transfer **120**, 735 (1998).
[12] J.-Y. Lee, H.-C. Park, J.-Y. Jung, and H.-Y. Kwak, J. Heat Transfer **125**, 687 (2003).
[13] J.-H. Tsai and L. Lin, J. Heat Transfer **124**, 375 (2002).
[14] W. D. Cooper, *Electronic Instrumentation and Measurement Techniques*, 2nd Ed. (Prentice Hall, Englewood Cliffs, NJ, 1978).
[15] J. P. Holman, *Experimental Methods for Engineers*, 6th Ed. (McGraw-Hill, New York, 1994).
[16] L. Lin and A. P. Pisano, Proceedings of the Micromechanical Sensors, Actuators, and Systems ASME, 1991, DSC-Vol. 32, pp. 147–163.
[17] J.-Y. Lee, H.-C. Park, J.-Y. Jung, and H.-Y. Kwak, J. Heat Transfer **125**, 687 (2003).
[18] V. P. Carey, *Liquid-Vapor Phase-Change Phenomena* (Hemisphere, Washington, D.C., 1992).

Downloaded 10 Aug 2007 to 147.46.245.171. Redistribution subject to AIP license or copyright, see http://jap.aip.org/jap/copyright.jsp